

# Fermi Bubble as a Source of Cosmic Rays in the Energy Range $> 10^{15}$ eV

K.-S. Cheng<sup>1</sup>, D. O. Chernyshov<sup>1,2,3</sup>, V. A. Dogiel<sup>1,2,3</sup>, C.-M. Ko<sup>1,3,0</sup>, W.-H. Ip<sup>3</sup>, and Y.  
Wang<sup>1</sup>

<sup>1</sup>Department of Physics, University of Hong Kong, Pokfulam Road, Hong Kong, China

<sup>2</sup>I.E.Tamm Theoretical Physics Division of P.N.Lebedev Institute of Physics, Leninskii pr.  
53, 119991 Moscow, Russia

<sup>3</sup>Institute of Astronomy, National Central University, Jhongli 320, Taiwan

December 3, 2024

Received \_\_\_\_\_; accepted \_\_\_\_\_

---

<sup>0</sup>cmko@astro.ncu.edu.tw

## ABSTRACT

Fermi-LAT has recently discovered two giant gamma-ray-bubbles which extend in the North and South of the Galactic center with diameter and height of the order of  $H \sim 10$  kpc. We suggest that periodic star capture processes by the galactic supermassive black hole, Sgr A\*, with a capture rate  $\tau_{cap}^{-1} \sim 3 \times 10^{-5} \text{ yr}^{-1}$  and energy release  $W \sim 3 \times 10^{52}$  erg per capture can produce hot plasma injecting into the Galactic halo at a wind velocity  $u \sim 10^8$  cm/s. The periodic injection of hot plasma can produce a series of shocks. Energetic protons in the Bubble are re-accelerated when they interact with these shocks. We show that for energy larger than  $E > 10^{15}$  eV, acceleration process can be better described by the stochastic second order Fermi acceleration.

We propose that hadronic CRs within the “knee” of the observed CR spectrum are produced by Galactic supernova remnants (SNRs) distributed in the Galactic disk. Re-acceleration of these particles in the Fermi Bubble produces CRs beyond the “knee”. With a mean cosmic ray diffusion coefficient in this energy range in the Bubble  $D_B \sim 3 \times 10^{30} \text{ cm}^2/\text{s}$ , we can reproduce the spectral index of the spectrum beyond the “knee” and within. Moreover, the conversion efficiency from shock energy of the Bubble into CR energy is about 10%. This model provides a natural explanation about the observed CR flux, spectral indices and matching of spectra at the “knee”.

*Subject headings:* Galaxy: halo - galaxies: jets - acceleration of particles - shock waves

## 1. Introduction

Recent discovery of a pair of giant Fermi Bubbles in the Galactic center (GC) is one of the most remarkable events in astrophysics. Using special procedure of background subtraction of Fermi-LAT data Su et al. (2010) found a pair of symmetric structure above and below the Galactic plane in the Galactic center direction. The origin of the bubble, if its existence will be proved, is still enigmatic and up to now a few models were presented in the literature. The team, which subtracted this structured gamma-ray emission from the total diffuse galactic emission, presented different explanations of the phenomenon though they seemed to tend towards the model of a single huge energy release in the Galactic center when, about 10 Myr ago, a huge cloud of gas or a star cluster was captured by the central supermassive black hole that produced the Fermi Bubbles we seen today.

Similar explanation was suggested by Guo & Mathews (2011) and Guo et al. (2011). They assumed that the Fermi bubbles can be created with a recent AGN jet activity about 1 – 2 Myr ago, which was active for a duration of  $\sim 0.1 - 0.5$  Myr, releasing a total energy of  $\sim 1 - 8 \times 10^{57}$  erg. The bipolar jets were ejected into the Galactic halo along the symmetric axis perpendicular to the Galactic plane.

It is important to note that the existence of the bubbles was first evidenced in X-rays detected by ROSAT as a narrow envelope with very sharp edges (Bland-Hawthorn & Cohen 2003) and later WMAP detected an excess of radio signals at the location of the gamma-ray bubbles (Finkbeiner 2004). The ROSAT structure is explained as a fast wind with a velocity  $u_w \sim 10^8$  cm/s is driving a shock into the halo gas. This phenomenon requires an energy release of about  $10^{55}$  ergs at the GC and this activity should be periodic on a timescale of the order of 10 Myr. This requirement of energy release in the GC is consistent with the observations of the existence of hot plasma with temperature about 10 keV in the Galactic Center (GC) region but of a radius of 30 – 50 pc only. This cannot be confined

and will escape from the GC with speed  $u_w \sim 10^8$  cm/s (Koyama et al. 2007). Therefore, sources with a power about  $10^{41}$  erg/s are required to heat the plasma or releasing  $\sim 10^{55}$  ergs from the GC in the past 10 Myr. However, Crocker & Aharonian (2011) proposed a relatively slow energy release ( $\sim 10^{39}$  erg/s) from supernova explosions as a source of proton production in the GC. The observed gamma-rays come from hadronic processes of the protons in the halo. The plasma in the halo is extremely turbulent and the protons are trapped for a time comparable to the Hubble time. But this model requires a separated origin of electrons, which has a much shorter life time than protons, to explain the WMAP data.

Intensive energy release has been observed, indeed, at the center of normal galaxies as strong variations of X-ray radiation. There are common characteristics of these X-ray sources. First, all these sources have been bright sources, and their X-ray luminosity could go up to about  $10^{44}$  erg/s. Second, they have shown a high level of variability in their X-ray light curve within years. In the “high state”, the luminosity of one source could be at least 100 times higher than its luminosity in its “low-state”. Third, most of them have a super soft spectrum during the flare, with effective black body temperatures of only about 10 – 100 eV (Komossa & Bade 1999; Halpern et al. 2004). The classic examples that satisfy these characteristics are RX J1624.9+7554, RX J1242.6-1119A, RX J1420+5334, RX J1331-3243, and NGC 5905. Many scenarios have been proposed to explain these phenomena. However, most of them fail to explain some of the observed results. A detailed discussion of these scenarios can be found in Komossa & Bade (1999). Among all the listed models, the tidal disruption model is the most commonly accepted model, and it gives the most satisfactory explanation to the observations by considering the radiation from the disk. In this model, when a star passes by a black hole within a capture radius, where the black hole tidal force becomes stronger than the self-gravity of the star, the star could be captured. The detailed capture and disruption process of a main-sequence star has been

studied by several authors (e.g. Rees 1988; Cannizzo et al. 1990). The capture rate of main sequence stars in our galaxy and in other galaxies as well is about  $10^{-4} \text{ yr}^{-1}$  to  $10^{-5} \text{ yr}^{-1}$  (see Syer & Ulmer 1999; Alexander 2005). Recently more stellar capture events have been observed (e.g. Esquej et al. 2008; Gezari et al. 2008, 2009; Komossa & Bade 1999; Cappelluti et al. 2009). Dynamical studies of nearby galaxies suggest that most if not all galaxies with a bulge component host a central supermassive black hole, and that the bulge and black hole mass are tightly correlated (Magorrian et al. 1998; Tremaine et al. 2002; Greene & Ho 2007).

The BAT on board of Swift has identified a transient X-ray source called GRB110328A (Cummings et al. 2011) with optical identification later (Cenko et al. 2011; Leloudas et al. 2011), which is located in the direction of constellation of Draco when it erupted in a series of X-ray flares. The distance to this source is determined to be  $z \sim 0.35$  by using  $H_\beta$  and OIII emission lines by Gemini Telescope (Levan et al. 2011a). The characteristics of GRB 110328A appear inconsistent with that of a gamma-ray burst (Barthelmy et al. 2011). In fact its time depending characteristics including various time scales in light curve, multi-wavelengths etc. seem to be better explained in term of the tidal disruption of a star by a supermassive black hole (Almeida 2011; Bloom et al. 2011; Levan et al. 2011b; Burrows et. al. 2011; Zauderer et al. 2011). All these recent observations suggest that stellar capture processes are quite common in other normal galaxies.

Observations have also reveal many evidences of unusual processes occurring in the central region of our Galaxy. For instance, the enigmatic 511 keV annihilation emission discovered by INTEGRAL (see e.g. Knoedlseder et al. 2005) which origin is still debated. The hot plasma with temperature about 10 keV which cannot be confined in the GC and, therefore, sources with a power about  $10^{41} \text{ erg/s}$  are required to heat the plasma (see Koyama et al. 2007, and references therein). In fact plasma outflows with velocity  $\gtrsim 10^7$

cm/s are observed from the nuclear region of our Galaxy (see Crocker et al. 2010) and from the nucleus of Andromeda (Bogdan & Gilfanov 2010). Time variations of the 6.4 keV line and X-ray continuum emission observed in the direction of molecular clouds in the GC which are supposed to be a reflection of a giant X-ray flare occurred several hundred years ago in the GC (see Inui et al. 2009; Ponti et al. 2010; Terrier et al. 2010, and references therein). HESS observations of the GC in the TeV energy range indicated an explosive injection of CR there which might be associated with the supermassive black hole Sgr A\* (e.g. Aharonian et al. 2006).

In a series of papers (Cheng et al. 2006, 2007; Dogiel et al. 2009a,b,c, 2011), we developed a model of energy release in the Galactic center due to star accretion onto the central black hole for the interpretation of X-ray and gamma-ray emission from the GC. Our goal was to explain these observational data in the framework of a single model. Basic assumptions in these models are (1) the galactic supermassive black hole Sgr A\* can capture a star in rate of  $\nu_s \sim 10^{-4} - 10^{-5} \text{ yr}^{-1}$  and (2) the energy release from each capture in the form of a flux of subrelativistic protons is  $W \sim 4 \times 10^{52} M_*^2 R_*^{-1} M_{\text{bh}}^{1/3} (b/0.1)^{-2} \text{ erg}$ , where  $M_*$  (in unit of  $M_\odot$ ) and  $R_*$  (in unit of  $R_\odot$ ) are the mass and the radius of the captured star,  $M_{\text{bh}}$  (in unit of  $10^6 M_\odot$ ) of the supermassive black hole and  $b$  is the ratio of the periapse distance  $r_p$  to the tidal radius  $R_T$  (see the review of Alexander 2005). In a time scale much longer than the capture time scale this model can be treat to have an average power injection  $\dot{W} \sim 3 \times 10^{40} \text{ erg/s}$ . These protons heat the surrounding plasma by Coulomb losses to 10 KeV.

Based on this model Cheng et al. (2011) (CCDKI model) argued that up to several hundred capture events might occur in the past 10 Myr, which generate a series of shocks propagating through the central part of the Galactic halo and thus produce accelerated relativistic electrons responsible for the bubble emission. Processes of charged particle

acceleration by the bubble shocks in terms of sizes of the envelope, maximum energy of accelerated particles, etc. may differ significantly from those obtained for SNe. In this paper we study if a “signal” from charged particles accelerated in the bubble region can be seen in the spectrum of cosmic rays observed at Earth. We present simple estimations of hadronic CR acceleration by the Fermi Bubble shocks up to energies above  $10^{15}$  eV. The paper is organized as follows. In section 2, we review current understanding about CR acceleration by SNRs and conclude that this process can only produce CRs with energies less than  $10^{15}$  eV. We present a simple solution of the multiple-shock structure in the halo in section 3. In section 4 we discuss the protons accelerated by the Bubble shocks. We emphasize that a broken power-law of particle distribution must be formed because of the finite spacing between consecutive shocks and the spectral break naturally occurs at  $10^{15}(u/10^8 \text{ cm/s})(l_{sh}/30 \text{ pc})(B/5 \mu\text{G})$  eV. Charged particles below and above this critical energy are accelerated by two different acceleration mechanisms. In section 5, we calculate the total particle spectrum by summing up the contribution from all shocks in the Bubble and compare it with the observed hadronic CR spectrum with energies larger than  $10^{15}$  eV. In section 6, we suggest a model that can produce the CR spectrum within and beyond the “knee” (around  $3 \times 10^{15}$  eV). Summary and discussion are presented in section 7.

## 2. CR Acceleration by SNRs in the Galaxy

From a general point of view SN explosions are enough to supply the power needed for the luminosity of CRs in our Galaxy,  $L_{CR} \sim 10^{41}$  erg/s (for a general review see Berezhko et al. 1994; Reynolds 2008). Diffusive shock acceleration (see Krymskii 1977; Bell 1978) is considered to be a viable and natural mechanism for cosmic ray accelerated by SNRs. The mechanism produces a power-law spectrum with the necessary spectral index that is observed experimentally. The simplest one-dimensional kinetic equation describing

this process has the form

$$\frac{\partial f}{\partial t} + \frac{\partial}{\partial z} \left( u(z)f - D \frac{\partial f}{\partial z} \right) - \frac{1}{3p^2} \frac{du(z)}{dz} \frac{\partial}{\partial p} (p^3 f) = 0, \quad (1)$$

where  $z$  is the coordinate perpendicular to the shock front,  $p$  is the particle momentum,  $u(z)$  is the velocity distribution which describes a velocity jump at the shock, and  $D$  is the spatial diffusion coefficient. The solution of this equation is a power-law function,  $f(p) \propto p^{-\gamma}$ , in which the spectral index  $\gamma$  is a function of the velocity jump at the shock. For strong shocks with Mach number much larger than unity,  $\gamma = 4$ . The corresponding energy spectral index is  $\nu = 2$  ( $N(E) \propto E^{-\nu}$ ).

The current status of the observations of middle-aged SNRs by LAT abroad of *Fermi* with energy range from 0.2 – 100 GeV has provided some insight of the shock-acceleration theory of SNRs (Castro & Slane 2010; Uchiyama 2011). Assuming the gamma-rays are produced by hadronic processes, Castro & Slane (2010) deduced the spectral index of 4 SNRs ranging between 2.1 – 2.4. However, whether the observed GeV gamma-rays are produced by hadronic processes or leptonic processes are very difficult to differentiate. On the other hand the ambiguity can be removed if broadband emissions are observed. In particular if GeV and TeV spectra can be described by a single power law, which is steeper than  $E^{-2}$ , the hadronic processes could be the more favorable mechanisms. Currently about 10 SNRs have been detected in both GeV and TeV bands, among them Tycho and CTB37A, whose GeV-TeV gamma-ray emission shows a uniformly steep spectral indices about 2.3 and 2.2, respectively (cf. Table 1 of Caprioli 2011). All these recent observations are consistent with conventional supernova shock acceleration theories, which suggest that the spectrum of cosmic rays is roughly described by  $E^{-2}$ .

Many fundamental questions related to the assumption of SNRs being the sources of the Galactic cosmic rays are still open. The maximum energy of the accelerated particles is the main concern for this scenario, which can be roughly estimated from a very simple



relation. The acceleration time at the shock is  $\tau_{acc}(E) \sim D(E)/u_{sh}^2$ , where  $u_{sh}$  is the shock velocity ( $\sim$  a few  $10^8$  cm/s). The minimum value of the diffusion coefficient at the shock follows from the Bohm diffusion scenario, i.e.  $D_{Bohm}(E) = (c/3)r_L(E)$  where  $r_L$  is the Larmor radius of the particle. Equating the acceleration time with the lifetime of the shock  $T$  we get an estimate for the maximum energy of accelerated particles after time  $T$

$$E_{max} \sim Ze\beta_{sh}u_{sh}BT, \quad (2)$$

where  $\beta_{sh} = u_{sh}/c$ ,  $B$  is the magnetic field strength at the shock. The combination  $u_{sh}B/c$  can be interpreted as an effective electric field.

For a supernova remnant of typical age  $\tau_{SNR} \sim 1000$  yr, the maximum energy of protons is easily estimated by requiring that the acceleration time remains smaller than  $\tau_{SNR}$ . Lagage & Cesarsky (1983) and Berezhko & Völk (2000) demonstrated that the maximum energy of protons within the scenario of Bohm diffusion is as large as  $E_{max} \sim 10^{13} - 10^{14}$  eV for standard galactic SNRs. Berezhko et al. (1994) estimated the efficiency of acceleration when a feedback reaction of accelerated particles on the front structure was included and they showed that in the Bohm limit CRs absorb about 20% of the explosion energy. The acceleration process acts as an effective viscosity in widening the region of the shock velocity jump and eventually the acceleration process stops.

However, outside the quasi-linear model the acceleration of cosmic rays at the shock fronts of SNRs may make the acceleration of particles more effective. As Bell (2004) (see also Bykov et al. 2009) showed that during acceleration at shocks of SNR, the magnetic non-resonant fluctuations were strongly driven. A non-linear MHD simulation indicated that CR-excited turbulence could amplify the magnetic field. It appears that acceleration to the spectral break at  $10^{15}$  eV normally ceases as SNR enters the Sedov phase. Thus, CR acceleration by SN shocks can only provide particles with the energies less than  $10^{15}$  eV.

The spectral index of the observed CR flux changes from 2.7 to 3.1 around energy  $10^{15}$

eV, and this is known as the “knee”. Standard model of CR acceleration by SN shocks cannot explain CR energies above the “knee”, because it only produces a single power-law spectrum up to the energy around  $10^{15}$  eV. In addition, the CR spectrum flattens again for energies above  $10^{18}$  eV, and this is known as the “ankle”. Large size is required to accelerate and to confine charged particles above “ankle” (the Larmor radius at these energies is comparable with the halo height). The origin of CRs above the ankle is generally attributed to extragalactic origin because those particles could not be confined inside the Galaxy and known potential galactic accelerators could hardly accelerate particles to such high energies.

The origin of the steepening for  $E \gtrsim 10^{15}$  eV is still an open question and different mechanisms of CR acceleration in the range  $10^{15} - 10^{18}$  eV in the Galaxy have been proposed. Ptuskin et al. (2010) assumed that the CR flux with energies above  $10^{15}$  eV is produced by very young galactic SNRs. They modelled the particle acceleration by spherical shocks with back reaction of cosmic-ray pressure on the shock structure. The significant magnetic field amplification in young SNRs produced by cosmic ray streaming instability may lead to a flux of CRs with the maximum energy of accelerated particles about  $5 \times 10^{18}$  eV. In this model the steepening of the CR spectrum at the knee position is due to distortion of the spectrum ejected from young SNRs by propagation process.

Another interpretation was suggested by Erlykin & Wolfendale (2006); Erlykin et al. (2010); Lagutin et al. (2008) who assumed that CRs at the knee were produced by a single, recent local supernova. Recently Butt (2009) summarized problems (including energies within the “knee”) of the conception that isolated SNRs are the main accelerators of CRs and discussed alternative scenarios of CR acceleration.

The reason of the steepening of CR spectrum at high energies may also be the result of a change in properties of diffusion in the interstellar medium. This effect of propagation

was mentioned first by Syrovatskii (1971) who noticed that the standard diffusion of CRs in the interstellar medium might be changed by convection due to a drift of these particles in the large scale galactic magnetic fields. This model was developed in Ptuskin et al. (1993) who assumed two types of CR diffusion in the Galaxy: the usual diffusion due to particle scattering on fluctuations of random magnetic fields and the Hall anisotropic diffusion (drift motion) due to the large scale galactic magnetic field whose effect might become important just above the knee energy.

As an alternative model, Jokipii & Morfill (1987) suggested a mechanism of acceleration in the Galaxy of ultra-high energy cosmic rays in a galactic wind and its hypothetical termination shock. In this scenario SNRs accelerate the bulk of cosmic rays up to  $10^{15}$  eV. These particles are further accelerated up to  $10^{19} - 10^{20}$  eV at a termination shock which is at a distance of a few hundred kpc from the disk. Ip & Axford (1992) analyzed multiple interaction of particles with SNRs in the Galactic disk as a source for CR acceleration above the knee. However, too many shocks are required in the disk in order to produce CR flux at the knee. However, Bykov & Toptygin (1993) showed that regions of CR acceleration to energies above  $10^{15}$  eV might be OB associations where concentration of shock fronts is very high. We will discuss this model in section 4.

In summary, it is generally agreed that SNR shocks can only accelerate particles to energies less than  $10^{15}$  eV. On the other hand, accretion processes in the GC may generate giant shocks which are effective for particle acceleration above  $10^{15}$  eV.

### 3. Structure of Shocks in the Fermi Bubble

As it was assumed in CCDKI the central massive black hole captures a star every  $\tau_{cap} \sim 3 \times 10^4$  years, and as a result about  $W \sim 3 \times 10^{52}$  ergs of energy in the form of

subrelativistic particles is released. This heats up the surrounding gas in the central region of our Galaxy. The hot gas expands into the halo and forms propagating upward shock. The situation is very similar to that of the stellar wind of a massive star blowing into its surrounding medium (see e.g. Weaver et al. 1977; Bisnovatyi-Kogan & Silich 1995).

The gas distribution in the disk and in the halo was derived in Cordes et al. (1991) and it can be presented as a double exponential distribution

$$n(\rho, z) = 0.025 \exp\left(-\frac{z}{1 \text{ kpc}}\right) \times \exp\left[-\left(\frac{\rho}{20 \text{ kpc}}\right)^2\right] + 0.2 \exp\left(-\frac{z}{0.15 \text{ kpc}}\right) \times \exp\left[-\left(\frac{\rho - 4 \text{ kpc}}{2 \text{ kpc}}\right)^2\right] \text{ cm}^{-3}. \quad (3)$$

The energy release in the GC due to star capture can be either impulsive or continuous depending on the characteristic times of star capture and energy dissipation of subrelativistic protons (plasma heating by Coulomb losses). The capture time is roughly  $\tau_{cap} \sim 3 \times 10^4$  yr and the dissipation time  $\tau_{diss}$  in the CCDKI model is determined by the rate of ionization losses of protons injected with the energy  $E_p$ , which is given by

$$\tau_{diss} \simeq 10^6 \left(\frac{n}{1 \text{ cm}^{-3}}\right)^{-1} \sqrt{\frac{E_p}{100 \text{ MeV}}} \text{ yr}, \quad (4)$$

where  $n$  is the gas density in vicinity of the GC which can be quite high (see discussion in Cheng et al. 2007), e.g., in nearby molecular clouds  $n > 10^4 \text{ cm}^{-3}$ .

If  $\tau_{cap} \ll \tau_{diss}$  we have the case of stationary energy injection in the GC. In this case the the region of heated gas is bounded by a single shock (see Weaver et al. 1977). For  $\tau_{cap} \gg \tau_{diss}$  a multi-shock structure is formed in the halo with shocks of different ages. A similar multi-shock structure can also be created if in the GC there are epochs of high frequency star captures. Thus, the number of shocks is determined by the injection and dissipation parameters.

For a highly simplified case of the exponential atmosphere with the scale height  $z_0$ , i.e.,

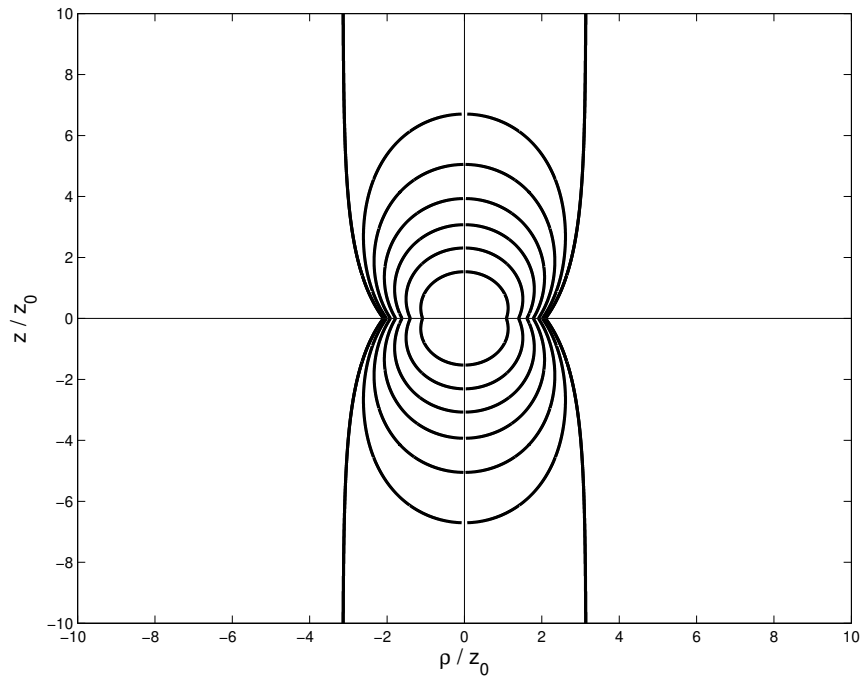


Fig. 1.— Multi-shock structure in the Bubble from the Kompaneets' solution. Seven representative shocks are shown.

the plasma density  $n(z) = n_0 \exp(-z/z_0)$ , an analytic solution of shock propagation was obtained by Kompaneets (1960) (see also the review of Bisnovatyi-Kogan & Silich 1995). This solution gives a qualitative picture of the shock propagation and parameters of the medium bounded by the shock that roughly described the situation expected in the Fermi Bubble. If the rate of energy injection is  $L$  then the radius of the shock as a function of the height  $z$  and the time  $t$  is

$$\rho(z, t) = 2z_0 \arccos \left\{ \frac{1}{2} \exp \left( \frac{z}{2z_0} \right) \left[ 1 - \left( \frac{y}{2z_0} \right)^2 + \exp \left( -\frac{z}{z_0} \right) \right] \right\}. \quad (5)$$

Here  $z$  is the coordinate perpendicular to the Galactic plane,

$$y = \int_0^t \left[ \frac{(\gamma_p^2 - 1)}{2} \frac{\lambda L t}{V(t) m n_0} \right]^{1/2} dt, \quad (6)$$

$V(t)$  is the current volume enveloped by the shock

$$V(t) = 2\pi \int_0^{a(t)} \rho^2(z, t) dz, \quad (7)$$

$a(t)$  is the position of the top of the shock

$$a(t) = -2z_0 \ln \left( 1 - \frac{y}{2z_0} \right), \quad (8)$$

$L = W/\tau_{cap}$  is the average luminosity of the central source,  $\gamma_p$  is the polytropic coefficient, and  $\lambda$  describes the fraction of explosion energy converted into the thermal energy of gas (see Bisnovatyi-Kogan & Silich 1995). As it follows from Eqs. (5) & (8), for the finite time  $t_1$  determined from the condition  $y(t_1) = 2z_0$  the shock breaks through the exponential atmosphere and the bubble top  $a(t_1)$  tends to infinity while the bubble radius in the Galactic plane ( $z = 0$ ) tends asymptotically to  $\rho = 2z_0 \cos^{-1}(1/2) \simeq 2z_0$  and for  $z \gg z_0$  to  $\rho \simeq \pi z_0$ .

A numerical solution of the system Eqs. (5) - (8) in dimensionless coordinates for shock waves at different ages is shown in Fig. 1. This figure is meant to be illustrative only. In

reality the distribution of shocks should be far more complicated. Neglecting the thin 4 kpc torus component of Eq. (3), the scale height of the ‘atmosphere’ is  $z_0 = 1$  kpc. The shock distribution in Fig. 1 is suggestive of a cylindrical bubble with an edge at a radius  $\rho_B \simeq 3$  kpc.

Base on this we put forward a quasi-stationary model of the Fermi Bubble which we regard as the source of hadronic cosmic rays with energy larger than  $10^{15}$  eV. The essence of the CCDKI model is energy is quasi-periodically injected into the halo when the stellar capture processes take place and may exist with a time scale comparable with the age of Milky way. Consequently, the Fermi Bubble should have a stationary structure. The idealized Kompaneets’ solution above shows that there is a stationary sideways boundary for shocks. For quasi-periodic star capture, the bubble interior is filled with shocks propagating in series and eventually stopping at  $\rho_B \simeq 3$  kpc. However, in the Kompaneets’ solution dissipation processes are ignored. The realistic situation has to be described by a set of dissipative hydrodynamic equations, which takes into account of the shocks propagation in non-uniform medium and various dissipation processes including shock heating, energy transfer into cosmic rays, slowing down due to accumulation of material, etc.. In fitting the observed gamma-ray spectrum, Cheng et al. (2011) concluded that electrons should have an escape time scale of 15 Myr in order to explain the spectral break position. The characteristic dissipation time scale of the shocks should be of the same order if these electrons are transported away by the shocks. The shocks will be pretty much dissipated away when they arrive at the sideways boundary ( $\rho_B$ ). There will be no pile up of shocks at  $\rho_B$ . As the speed of shocks along the Bubble axis is progressively larger than the sideways speed, the upper and lower boundaries of the Bubble will be the same as the halo boundary ( $z = \pm H = \pm 10$  kpc from the mid-plane). Thus the Bubble has a stationary structure.

Same result for the dimension of the Bubble can be obtained if we use the swept up

mass model proposed by Cheng et al. (2011). In this model the radius of the sideways shock front or the swept-up front is given by  $\rho_s = \sqrt{2\lambda W / \pi m n \Delta z u_{s\rho}^2}$ , where  $u_{s\rho}$  is the speed of the sideways shock front (or swept-up front) and  $\Delta z = u \tau_{cap}$ . With  $u \sim 10^8$  cm/s,  $\tau_{cap} \sim 3 \times 10^4$  yr,  $\Delta z \sim 30$  pc. We argue that the sideways shock front or swept-up front would disappear when its speed is smaller than the local sound speed. In Cheng et al. (2011) we have estimated that the shocks heat up the halo to  $\sim 1$  keV and the characteristic sound speed is of the order of  $v_s \sim 3 \times 10^7$  cm/s. Thus putting  $u_{s\rho} \sim v_s$ , the sideways boundary  $\rho_B \approx 3.2 \text{ kpc} (\lambda W / 2 \times 10^{52} \text{ erg})^{1/2} (\Delta z / 30 \text{ pc})^{-1/2} (n / 10^{-3} \text{ cm}^{-3})^{-1/2} (v_s / 3 \times 10^7 \text{ cm/s})^{-1}$  (note that  $\lambda W$  is the fraction of injected energy converted into thermal energy of gas).

#### 4. Proton Acceleration by the Bubble Shocks

Correct analysis of shock acceleration in the Bubble requires sophisticated calculations of each stage of this process which we hope to perform latter on. Now we present simple estimates of the characteristics of the spectra of the accelerated particle in the framework of the CCDKI model.

Below we analyze the spectrum of protons accelerated in the Bubble and discuss whether the Bubble contribution into the total flux of CRs in the Galaxy may explain the “knee” steepening. We remind that the generally accepted point of view is that the flux of relatively low energy CRs ( $< 10^{15}$  eV) is generated by SNRs, which eject a power-law spectrum  $E^{-2}$  into the interstellar medium. This spectrum is steepened by propagation (escape) processes in the Galaxy in accordance with the spectrum observed near Earth (see for details Berezhinskii et al. 1990). However these sources can hardly produce CRs with energies  $> 10^{15}$  eV, at which a steepening (the “knee”) in the CR spectrum is observed. For characteristics of the knee spectrum and models of its origin see the review of Kotera & Olinto (2011). We suggest that the Bubble could generate the flux of CRs at



energies  $> 10^{15}$  eV because the shocks in the Bubble have much larger length scales and longer lifetime in comparing with those in SNRs.

In the framework of CCDKI the Bubble may fill with hundreds shocks propagating in series one after another, though a single shock structure cannot be excluded too. The average separation between two shocks is given by

$$l_{sh} = \tau_{cap} u = 30 \left( \frac{\tau_{cap}}{3 \times 10^4 \text{ yr}} \right) \left( \frac{u}{10^8 \text{ cm/s}} \right) \text{ pc}, \quad (9)$$

However the exact separation between two consecutive shocks depends on the actual time separation of two consecutive capture events and their energy releases. There is another important spatial scale which characterizes processes of particle acceleration by a single shock: the diffusion length scale at a single shock  $l_D \sim D/u$ .  $u$  is the shock velocity, and  $D$  is the spatial diffusion coefficient of the energetic particles near a shock which depends on particle interaction with small scale magnetic fluctuations. In Bohm limit,  $D \sim cr_L(E)/3$ , where  $r_L(E) = E/ZeB$  is the particle Larmor radius. In this case

$$l_D \sim \frac{cr_L}{u} = \frac{cE}{ZeBu}. \quad (10)$$

The problem of particle acceleration in conditions of supersonic turbulence (multiple-shock structure) was extensively analysed before (e.g. Spruit 1988; Achterberg 1990; Schneider 1993; Melrose & Pope 1993) as well as quasi-periodic flows (e.g. Webb et al. 2003). In a series of papers by Bykov & Toptygin (1993); Bykov & Fleishman (1992); Bykov & Toptygin (2001) the idea was applied to acceleration processes in OB associations, which is quite similar to the structure of the Bubble. They introduced a dimensionless parameter characterizing the acceleration regimes

$$\psi = \frac{l_{sh}}{l_D} \sim \frac{ul_{sh}}{D} \sim \frac{ul_{sh}}{cr_L}. \quad (11)$$

The critical energy  $E_1$  that separate two regimes of acceleration can be estimated from the condition  $\psi \sim 1$  or  $l_D(E_1) \sim l_{sh}$ . For the conditions of the Fermi Bubble the critical energy

is

$$E_1 \approx \frac{ZeBul_{sh}}{c} = 10^{15} Z \left( \frac{B}{5 \mu\text{G}} \right) \left( \frac{l_{sh}}{30 \text{ pc}} \right) \left( \frac{u}{10^8 \text{ cm}} \right) \text{ eV}. \quad (12)$$

In the case of  $\psi \gg 1$  or  $l_D \ll l_{sh}$ , the analysis in Bykov & Toptygin (1993); Bykov & Fleishman (1992) showed that there is a combined effect of a fast particle acceleration by a single shock, which generates the spectrum  $E^{-2}$  and relatively slow transformation of this spectrum due to interaction with other shocks (stochastic Fermi acceleration) into a hard  $E^{-1}$  spectrum in the intershock medium at relatively low energies. However it is unclear if such slow transformation can be completed within the life time of the shocks in the Bubble. Detailed numerical analysis is needed. Furthermore, from the general point of view the characteristic acceleration time is quite short in the range  $E \lesssim E_1$ , which is roughly given by the shock acceleration time  $cr_L/u^2$ . In the range  $E \gtrsim E_1$ , the acceleration time scale increases to the time of stochastic acceleration,  $cl_{sh}/u^2$ . With an average galactic spatial diffusion coefficient  $D_G$  outside the Bubble and a Galactic halo of height  $H$ , the characteristic escape time is  $\tau_{esc} \sim H^2/D_G$ . We expect that escape processes, which play a crucial role in determining the particle spectrum shown in our next analysis, are insignificant in the range  $E \lesssim E_1$ . Therefore the particle spectrum produced by the Bubble should be  $\sim E^{-\nu}$  for  $E < 10^{15}$  eV, where  $2 > \nu > 1$ . As discussed in section 2 SNRs are the major contributors for CRs with energies  $E \lesssim 10^{15}$  eV, the exact particle spectrum generated from the Bubble is unimportant in the energy range of  $E \lesssim 10^{15}$  eV.

In the case of  $\psi \ll 1$  or  $l_D \gg l_{sh}$ , inside the region of supersonic turbulence, the acceleration regime shifts to a pure stochastic acceleration by the supersonic turbulence. We extend the equation derived by Bykov & Toptygin (1993) for CR acceleration in supersonic turbulence in stationary state and axisymmetric geometry to include spatial dependent diffusion coefficient and external source,

$$\frac{\partial}{\partial z} \left( D(\rho, p) \frac{\partial f}{\partial z} \right) + \frac{1}{\rho} \frac{\partial}{\partial \rho} \left( D(\rho, p) \rho \frac{\partial f}{\partial \rho} \right) + \frac{1}{p^2} \frac{\partial}{\partial p} \left( \kappa(\rho, p) p^2 \frac{\partial f}{\partial p} \right) = -Q(\rho, z, p), \quad (13)$$

where  $\rho$  and  $z$  are the cylindrical spatial coordinates,  $p$  is the particle momentum.  $D(\rho, p)$  is the spatial diffusion coefficient and  $\kappa(\rho, p)$  is the momentum diffusion coefficient. Their spatial and momentum dependence in our model will be described below.  $Q(\rho, z, p)$  is the possible CR source which will be useful in our numerical example in section 6.

As we mentioned above, it is reasonable to assume that CRs with energies  $E \lesssim 10^{15}$  eV are supplied by SNRs. Therefore, in this section, we concentrate on the analysis of the acceleration of CRs in the energy range  $E \gtrsim E_1$  in the Bubble by supersonic turbulence. Later in section 6, we will treat the case with SNRs and Bubble and deal with energy from less than  $10^{12}$  eV to larger than  $10^{18}$  eV.

We set the boundary condition of the distribution function at the galactic halo outer boundary

$$f|_{\Sigma} = 0, \quad \text{at} \quad \rho = \rho_G \quad \text{and} \quad z = \pm H. \quad (14)$$

Proton acceleration in the Bubble depends sensitively on the acceleration parameters and structure of the Bubble. In the following we present a detailed analysis. We model the bubble region as a cylinder extending above and below the Galactic plane from  $z = 0$  to  $z = \pm H$  with a radius  $\rho = \rho_B$ . Assume there is no CR source inside the Bubble (i.e.,  $Q = 0$ ). The diffusion coefficients inside and outside the bubble are supposed to be different

$$D(\rho) = D_B \theta(\rho_B - \rho) + D_G \theta(\rho - \rho_B), \quad (15)$$

$$\kappa(\rho, p) = \kappa_B p^2 \theta(\rho_B - \rho), \quad (16)$$

where  $D_B \sim cl_{sh}/3$  is the coefficient inside the bubble due to interactions with a supersonic turbulence and  $D_G$  is the average diffusion coefficient in the Galaxy, e.g., defined in Berezhinskii et al. (1990). The momentum diffusion coefficient is  $\kappa_B \sim u^2/D_B$ . The momentum dependence of  $f$  can be represented by a power-law function,  $f(p) \propto p^{-\gamma}$ , where  $\gamma$  should be determined from Eq. (13).

To understand the dependence of  $\gamma$  on other parameters, we make two simplifications of Eq.(13), which do not affect the value of  $\gamma$  significantly. First, for  $H < \rho_G$ , as expected from Strong & Moskalenko (1998), particles escape through the radial boundaries at  $\rho = \rho_G$  are insignificant (see Berezhinskii et al. 1990), and we can shift the halo boundary to infinity, i.e.,  $\rho_G = \infty$ . Second, we model the axisymmetric geometry of the problem as planar geometry (i.e., we assume  $\partial f / \partial \rho \gg f / \rho$ ). We go back to the axisymmetric geometry afterward.

As in Bulanov et al. (1972) and Bulanov & Dogel (1974) we search solutions of Eq. (13) by the method of separation variables,  $f = R(\rho)Z(z)p^{-\gamma}$ . The solution for  $Z(z)$  has a very simple form

$$Z_n(z) = \cos(k_n z / H), \quad (17)$$

where  $k_n = \pi(n + 1/2)$ . We should point out that to make sure  $f$  is non-negative we must take  $n = 0$  for physical solutions.

To illustrate ideas, we consider the case  $D_G = D_B$  and approximate the axisymmetric geometry as planar (i.e.,  $d^2 R / d\rho^2 \gg 1/\rho dR/d\rho$ ). Using dimensionless variable  $\varrho = \rho/H$ , Eq. (13) can be simplified as

$$\frac{d^2 R}{d\varrho^2} - \left[ k_n^2 + \gamma(3 - \gamma) \frac{\kappa_B \theta(\varrho_B - \varrho) H^2}{D_B} \right] R = 0, \quad (18)$$

which has the exact form of the Schrödinger equation for a rectangular potential well:

$$\frac{d^2 \Psi}{d\varrho^2} + \frac{2m}{\hbar^2} (\mathcal{E} - U_0) \Psi = 0, \quad \text{for } 0 < \rho < \rho_B \quad (19)$$

and

$$\frac{d^2 \Psi}{d\varrho^2} + \frac{2m}{\hbar^2} \mathcal{E} \Psi = 0, \quad \text{for } \rho > \rho_B \quad (20)$$

when we define  $\mathcal{E}$  and  $U_0$  as

$$\mathcal{E} = -\frac{\hbar^2 k_n^2}{2m}, \quad \text{and} \quad U_0 = \frac{\hbar^2}{2m} \gamma(3 - \gamma) \frac{\kappa_B H^2}{D_B}. \quad (21)$$

The solution of this equation is well-known (e.g. Landau & Lifshitz 1991, Ch.3, §22):

$$\begin{aligned}
\Psi(\varrho) &= C_1 \exp(k_n \varrho) , \quad \text{for } \varrho < 0, \text{ where } k_n = \sqrt{-2m\mathcal{E}}/\hbar \\
\Psi(\varrho) &= C_2 \exp(-k_n \varrho) , \quad \text{for } \varrho > \varrho_B , \\
\Psi(\varrho) &= C \sin(\varsigma \varrho + \delta) , \quad \text{for } 0 < \varrho < \varrho_B , \text{ where } \varsigma = \sqrt{2m(\mathcal{E} - U_0)}/\hbar
\end{aligned} \tag{22}$$

From the continuity of the logarithmic derivative of  $\Psi$  at the well boundaries we have the condition

$$\arcsin\left(\frac{\hbar k_n}{\sqrt{-2mU_0}}\right) = \frac{(j\pi - k_n \rho_B)}{2} \tag{23}$$

and

$$\cos \xi = \pm \chi \xi , \quad \text{for odd } j , \tag{24}$$

$$\sin \xi = \pm \chi \xi , \quad \text{for even } j , \tag{25}$$

where

$$\xi = \frac{k_n \rho_B}{2} , \quad \text{and} \quad \chi = \frac{\hbar}{\rho_B} \sqrt{\frac{-2}{mU_0}} . \tag{26}$$

For strong acceleration,  $u^2 H^2 / D_B^2 \gg 1$ , Eqs. (24) & (25) determine a finite number of levels. From these equations, the first term of the series gives

$$\gamma = \frac{3}{2} + \sqrt{\frac{9}{4} + \frac{\pi^2 D_B}{\rho_B^2 \kappa_B}} \simeq 3 . \tag{27}$$

For weak acceleration,  $u^2 H^2 / D_B^2 \ll 1$ , we can use the shallow well solution presented in Landau & Lifshitz (1991). In this case there is only one level at  $E_0 \simeq U_0$  that gives

$$\gamma \simeq \frac{3}{2} + \sqrt{\frac{9}{4} + \frac{\pi^2 D_B}{H^2 \kappa_B}} \gg 1 . \tag{28}$$

A rough estimate of the power of CR production by the Bubble can be done in the same way as presented in Berezhinskii et al. (1990) for GeV CRs. The energy density of CRs

at  $E = 3 \times 10^{15}$  eV is  $n_{CR} \simeq 6.7 \times 10^{-17}$  erg cm $^{-3}$  (see Kotera & Olinto 2011). Then the power required for the Bubble to produce the knee at Earth is

$$W_B \sim \frac{cn_{CR}M_H}{x} \quad (29)$$

where  $M_H$  is the total mass of hydrogen in our Galaxy which is about  $10^{43}$  g and  $x$  is an extrapolation to energies  $> 10^{15}$  eV of the CR grammage derived from the chemical composition by Jones et al. (2001) up to energies about several hundred GeV,  $x(E) \sim 11.8 \times (4.9 \text{ GeV}/E)^{0.54}$  g/cm $^2$ . Then we obtain the required power of CR sources at the knee energy range  $W_B \sim 2 \times 10^{39}$  erg/s, which can easily be supplied by star capture processes.

More accurate values of  $\gamma$  can be derived from numerical calculation for the axisymmetric case:

$$\frac{1}{\varrho} \frac{d}{d\varrho} \left( \varrho \frac{dR_i}{d\varrho} \right) - \left[ k_n^2 + \gamma(3 - \gamma) \frac{\kappa_{Bi} H^2}{D_B} \right] R_i = 0, \quad (30)$$

Here the index  $i = 1, 2$  denotes region inside ( $\varrho < \varrho_B$ ) and outside ( $\varrho \geq \varrho_B$ ) the Bubble, respectively. Note that  $\kappa_{B1} = \kappa_B$  and  $\kappa_{B2} = 0$  (see Eq. (16)). A solution inside and outside the bubble is searched as series of the Bessel functions ( $J_\nu$ , inside the bubble) and the McDonald functions ( $K_\nu$ , outside the bubble).

The boundary conditions at the Bubble radius,  $\varrho = \varrho_B$  are:

$$R_1(\varrho_B) = R_2(\varrho_B), \quad \text{and} \quad D_B \left. \frac{dR_1}{d\varrho} \right|_{\varrho_B} = D_G \left. \frac{dR_2}{d\varrho} \right|_{\varrho_B}. \quad (31)$$

These relations can be satisfied if

$$\alpha_1 = k_n^2 + \gamma(3 - \gamma)\kappa_B H^2 / D_B < 0, \quad (32)$$

the above requirement implies  $\gamma > 3$ . For  $n = 0$  we have,

$$R_1(\varrho) = C_1 J_0(\sqrt{-\alpha_1} \varrho), \quad \text{and} \quad R_2(\varrho) = C_2 K_0(\pi \varrho / 2), \quad (33)$$

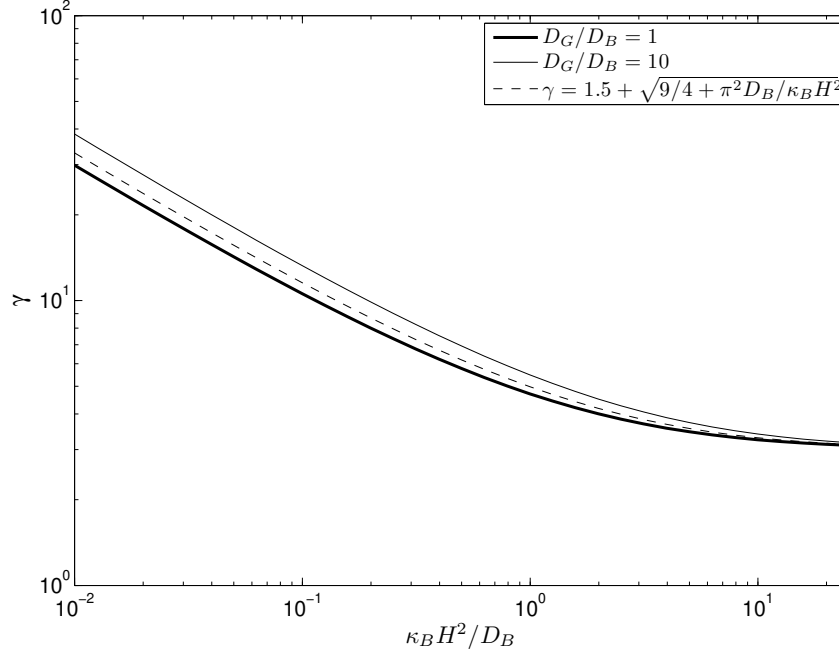


Fig. 2.— The spectral index for different acceleration rates.

or

$$\frac{D_B \sqrt{-\alpha_1} J_1(\sqrt{-\alpha_1} \varrho_B)}{J_0(\sqrt{-\alpha_1} \varrho_B)} = \frac{\pi D_G K_1(\pi \varrho_B/2)}{2K_0(\pi \varrho_B/2)}. \quad (34)$$

Numerical results of different ratios of  $D_G/D_B$  as a function of the ratio between the times of particle escape from the Galaxy  $H^2/D_B$  and the time of Fermi acceleration  $1/\kappa_B \sim D_B/u^2$  are shown in Fig. 2. The dashed curve shows the approximation estimate given by Eq.(28), which indicates that Eq.(28) is a good approximation and we will use it in the next section of data fitting for simplicity.

The spatial distribution of accelerated protons for different ratios  $D_G/D_B$  is shown in Fig. 3. We can see that these two distributions do not have a qualitative difference even if the ratios differ by a factor of 10.

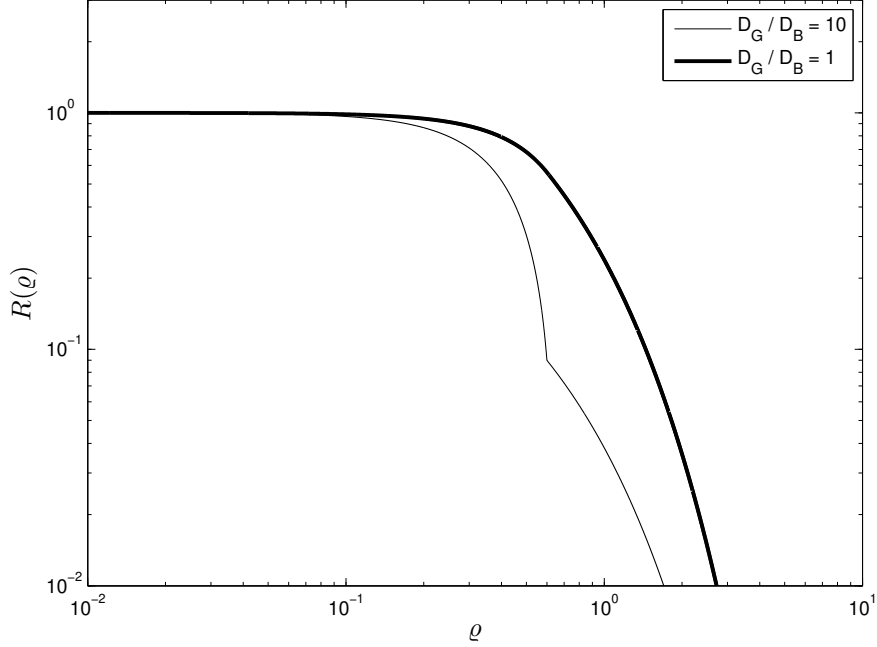


Fig. 3.— Spatial distribution of protons in the central region of the Galaxy as a function of  $\varrho$ . Here  $\varrho$  is normalized to  $H$  (the height of the halo), and in this example the Bubble boundary is taken as  $\varrho_B = 0.6$ .

### 5. Bubble Contribution to CRs at Energy Larger than $10^{15}$ eV

In this section we use the general models developed in last section to fit the cosmic ray spectrum for  $E > 10^{15}$  eV but we ignore any possible spectral modulation effect due to propagation from the Bubble to the Earth. We have shown that the charged particles in the Bubble can be described by a power-law spectrum,

$$\frac{d\dot{N}}{dE} = \frac{\dot{N}_0}{E_1} \left( \frac{E}{E_1} \right)^{-\nu}, \quad (35)$$

where  $E_1$  is given by Eq. (12) and  $\nu = \gamma - 2$ , which can be expressed as

$$\nu = -\frac{1}{2} + \sqrt{\frac{9}{4} + \frac{\pi^2 D_B^2}{u^2 H^2}}, \quad (36)$$



for  $E_1 < E < E_2$  where  $E_2$  is the high energy cutoff and will be discussed below. We have used the momentum diffusion coefficient  $\kappa_B = u^2/D_B$ . Here  $\dot{N}_0$  is a normalization constant which is chosen to fit the observed CR spectrum by assuming that the CR spectrum with energy  $E > 10^{15}$  eV is entirely contributed by particles from the Bubble.  $E_2$  can be estimated by Eq. (2), which gives

$$(E_2)_{min} \approx 3 \times 10^{17} \left( \frac{B}{5 \mu\text{G}} \right) \left( \frac{T}{10 \text{ Myr}} \right) \left( \frac{u}{10^8 \text{ cm/s}} \right)^2 \text{ eV}, \quad (37)$$

where  $T$  is the time taken by a single shock propagating from the disk to the top of the Bubble. However this estimate assumes that particles are only accelerated by a single shock. As described in previous section the high energy particles are accelerated by multiple shocks in the Bubble, in other words, particles can diffuse downward and continue to be accelerated by younger shocks in lower part of the Bubble. Therefore  $T \sim 10$  Myr is only a minimum life time, which means that the above estimate can be considered as the lower limit of  $E_2$ . Another possible way to restrict the maximum value of  $E_2$  is when the Larmor radius of the particles ( $r_L = E/eB$ ) is larger than the radius of the Bubble ( $H/2$ ),

$$(E_2)_{max} \approx 10^{19} \left( \frac{B}{5 \mu\text{G}} \right) \left( \frac{H}{10 \text{ kpc}} \right) \text{ eV}. \quad (38)$$

In fact this estimate should be more appropriate for  $E_2$  and we will use it in our model fitting process.

In our model particle spectrum there are four parameters: the lower cutoff  $E_1$  (Eq. (12)), the upper cutoff  $E_2$  (Eq. (38)), the spectral index  $\nu$  (Eq. (36)), and the normalization  $\dot{N}_0$  (Eq. (35)). We consider that  $l_{sh} = 30$  pc,  $B = 5 \mu\text{G}$ ,  $u = 10^8$  cm/s and  $H = 10$  kpc are very reasonable mean values in the Bubble, therefore in our model fitting we fix  $E_1 = 10^{15}$  eV and  $E_2 = 10^{19}$  eV. On the other hand the conversion efficiency from the shock energy into particle energy and the mean diffusion coefficient  $D_B$  in the Bubble are most uncertain parameters. Therefore in our model fitting we treat these two

parameters as fitting parameters. The solid line in Fig. 4 indicates the best fit. The best fit gives  $\nu = 3.12$ , which corresponds to  $D_B \sim 3 \times 10^{30} \text{ cm}^2/\text{s}$ . This is in agreement with the estimation  $D_B \sim cl_{sh}/3$  if we take the average separation between shocks as  $l_{sh} \sim 100 \text{ pc}$  (see Eq. (9)). This seemingly large diffusion coefficient is in fact at least an order of magnitude smaller than the coefficient in the halo for  $E > 5 \times 10^{15} \text{ eV}$  (e.g., Jones et al. 2001, suggested  $D_G \approx 2.0 \times 10^{28} (E/4.9 \text{ GeV})^{0.54} \text{ cm}^2/\text{s}$ ).

If the CRs in the energy range  $10^{15} \text{ eV} < E < 10^{19} \text{ eV}$  arriving at Earth come from the Bubble, then the power provided by the Bubble for CR in this energy range is given by  $\dot{W}_{CR} \approx \int_{10^{15} \text{ eV}}^{10^{19} \text{ eV}} 4\pi R^2 F_{CR}(E) dE \sim 3 \times 10^{39} (R/10 \text{ kpc})^2 \text{ erg/s}$ , where  $F_{CR}(E)$  is the observed CR energy flux and  $R$  is the mean distance to the Bubble. We find that the conversion efficient from shock power,  $\dot{W} \sim W/\tau_{cap} \sim 3 \times 10^{40} \text{ erg/s}$ , is about 10%, which is consistent with recent estimation by using Fermi-LAT data (Abdo et al. 2010). Realistically particles could escape from the Bubble through various locations of the Bubble’s surface, where the local strength of magnetic field maybe different. In addition we have pointed out that there are two possible ways to estimate the value of  $E_2$  (Eqs. (37) & (38)). Therefore it is likely that  $E_1$  and  $E_2$  coming out from the Bubble should have some distribution. In the dotted line in Fig. 4 we keep the spectral index as that of the solid line but assume that  $E_1$  and  $E_2$  have a uniform distribution between  $2 \times 10^{14} \text{ eV} < E_1 < 2 \times 10^{15} \text{ eV}$  (which corresponds to  $1 \mu\text{G} < B < 10 \mu\text{G}$ ), and  $(E_2)_{min} < E_2 < (E_2)_{max}$ , respectively. We can see that the model curve starts to drop around  $3 \times 10^{18} \text{ eV}$  and matches the data better. Furthermore we have argued that the injected spectrum from the shock is  $E^{-2}$  for  $E < E_1$  and slowly become harder to  $E^{-1}$  due to interactions with multiple shocks after sufficiently long time. However it is unclear if this spectral hardening process can be completed within the finite life time of the particles in the Bubble (see section 4 for more detail discussion). Therefore we cannot predict the exact spectral index for  $E < E_1$ . For reference purpose, in Fig. 4 we show these two possibilities: the dashed line for  $E^{-2}$  and the dash-dotted line for  $E^{-1}$ ,

respectively. Both  $E_1$  and  $E_2$  of these two lines also assume uniform distributions.

## 6. Model for High Energy CRs Within and Beyond the Knee

The observed high energy CR spectrum is a broken power law. The energy spectral index for CR energy smaller than the “knee” (around  $3 \times 10^{15}$  eV) is 2.7. The index increases to 3.1 for larger energy (until around  $10^{19}$  eV where the spectrum becomes harder again). The general argument is the sources (i.e., acceleration mechanisms and/or sites) responsible for the energy range within and beyond the “knee” should be different. The intriguing fact is that the two power laws match quite well at the “knee”. This coincident problem is difficult to sort out if the two sources are totally unrelated.

CRs within (i.e., energy less than) the “knee” are generally attributed to SNRs in our Galaxy (see section 2). In previous two sections, we alluded the acceleration site of CRs beyond the “knee” (i.e., energy larger than the “knee”) to the Fermi Bubble. In section 4, we studied Eq. (13) without source in the Bubble. The solution gave the characteristic spectrum of the system. In reality we need a source or a seed population for the Bubble. We deem that we do not need a new seed population for Bubble acceleration. Instead we propose the following model: some of the CRs produced by SNRs in the Galactic disk are re-accelerated in the Bubble to energy beyond the “knee”. This model has the potential of solving the coincident problem naturally, because the source of CRs beyond the “knee” is seeded by the source within the “knee”.

To consolidate our idea, we work out a concrete numerical model. Basically, we are going to solve the stationary state cosmic ray transport equation Eq. (13) in our Galaxy with two Fermi Bubbles (one on each side of the Galactic plane). We modelled our Galactic halo as a cylinder of radius  $\rho_G = 20$  kpc, and the top and bottom at  $\pm 10$  kpc from the

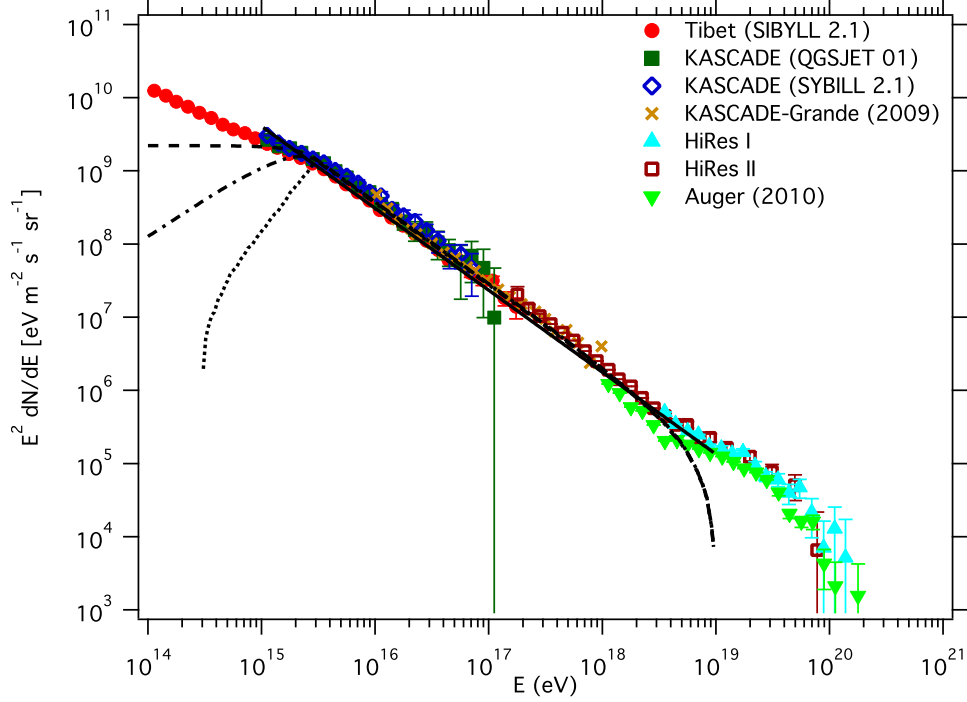


Fig. 4.— The Bubble contribution to the flux of CRs. The data is summarized in Kotera & Olinto (2011). The spectrum has been multiplied by  $E^2$  for clarity. Experiments include Tibet AS- $\gamma$  (Amenomori et al. 2008) KASCADE (Kampert et al. 2004), KASCADE-Grande (Apel et al. 2009), HiRes-I (Abbasi et al. 2009), HiRes-II (Abbasi et al. 2008), and Auger (Abraham et al. 2010). The solid line shows the contribution from the Bubble predicted by equation (34) for  $E_1 = 10^{15} \text{ eV} < E < E_2 = 10^{19} \text{ eV}$ . The dotted line has the same spectral index as that of the solid line but both  $E_1$  and  $E_2$  are assumed to obey a uniform distribution (see the text for explanation). The dashed line and the dash-dotted line have the same spectral index for  $E_1 < E < E_2$  and distribution of  $E_1$  and  $E_2$  as that of the dotted line except the spectral index changes to 1 and 2, respectively, for  $E < E_1$  (see the text for explanation).

mid-plane. Each Fermi Bubble is also a cylinder of the same height  $\pm 10$  kpc, but of a radius  $\rho_B = 3$  kpc.

The Fermi Bubbles are filled up with shocks as described in section 3 (see Fig. 1). The spatial diffusion coefficient are different inside and outside the Bubble as described by Eq. (15). Due to the very turbulent nature inside the Bubble, we consider a constant spatial diffusion coefficient and adopt  $D_B = 2.08 \times 10^{30}$  cm<sup>2</sup>/s (cf. estimate value by fitting process in section 5). Outside the Bubble, we take into account of the the energy (or momentum) dependence of the spatial diffusion coefficient and adopt  $D_G = D_0(pc/4 \text{ GeV})^{0.6}$ ,  $D_0 = 6.2 \times 10^{28}$  cm<sup>2</sup>/s (cf. Jones et al. 2001).

According to the analysis in section 4 the acceleration of energetic particles in the Bubble is facilitated by stochastic acceleration (second order Fermi acceleration). Assuming that there is little or no stochastic acceleration outside the Bubble, we model the momentum diffusion coefficient as a step function as in Eq. (16) and adopt  $\kappa_B H^2/D_B = 1.9$  (i.e.,  $\kappa_B = 4.4 \times 10^{-15}$  s<sup>-1</sup> or the corresponding acceleration time scale is 7.6 Myr).

The Galactic disk contains supernova remnants (SNRs). We adopt the distribution suggested by Stecker & Jones (1977) and modified it with a Gaussian thickness profile

$$Q_{\text{SNR}}(\rho, z) \propto \left(\frac{\rho}{R_\odot}\right)^{1.2} \exp\left(-\frac{3.22\rho}{R_\odot}\right) \exp\left(-\frac{z^2}{h^2}\right), \quad (39)$$

where  $\rho$  is the galactocentric radius and  $z$  is the distance perpendicular to the mid-plane. Here we take  $h = 100$  pc,  $R_\odot = 8$  kpc. We adopt that SNRs inject energetic particles in the form of power law with a high energy cutoff at  $p_{\text{max}}c \approx 3 \times 10^{15}$  eV. Therefore, together with the SNR distribution (Eq. (39)), the source function is

$$Q(\rho, z, p) = Q_0 \left(\frac{p}{p_{\text{max}}}\right)^{-\mu} \exp\left(-\frac{p}{p_{\text{max}}}\right) \left(\frac{\rho}{R_\odot}\right)^{1.2} \exp\left(-\frac{3.22\rho}{R_\odot}\right) \exp\left(-\frac{z^2}{h^2}\right). \quad (40)$$

As mentioned in section 2, we take the SNR injection spectrum to be  $\mu = 4.35$  (see also Biermann & Strom 1993). The normalization  $Q_0$  is obtained by fitting the simulation

result to the observed spectrum and the value is  $1.5 \times 10^{14}$  particles/s/kpc<sup>3</sup>/(GeV/c)<sup>3</sup>. Integrating  $Q(\rho, z, p)$  over the Galaxy and momentum (from 1 GeV/c to  $p_{max}$ ) gives the total luminosity of CRs  $4 \times 10^{40}$  erg/s, which is consistent with the value in literature (e.g., Berezhinskii et al. 1990).

Finally, the appropriate boundary conditions for the momentum coordinate are

$$\left. \frac{p}{f} \frac{\partial f}{\partial p} \right|_{p=p_{low}} = -4.7, \quad f|_{p=p_{up}} = 0, \quad (41)$$

where the energy of the lower momentum boundary is  $p_{low}c = 10^{12}$  eV, and the upper momentum boundary is  $p_{up}c = 3 \times 10^{18}$  eV. The condition at the lower momentum ensures the spectral index matches that of low energy CRs (say  $E < 10^{12}$  eV).

The spatial boundary conditions are

$$\left. \frac{\partial f}{\partial \rho} \right|_{\rho=0} = 0, \quad f|_{\rho=\rho_G} = 0, \quad (42)$$

where the radius of the Galactic disk was taken to be  $\rho_G = 20$  kpc.

$$\left. \frac{\partial f}{\partial z} \right|_{z=0} = 0, \quad f|_{z=\pm H} = 0, \quad (43)$$

where the height of the halo  $H = 10$  kpc.

The spectrum evaluated at the Earth’s position is solid line shown in Fig. 5. The model fits the data reasonably well and it is no coincident that the spectra join smoothly at the “knee”. For reference, in Figs. 6 & 7 we show the spatial distribution of CRs from our simulation. The labels ‘Low’ and ‘High’ refer to the number density of particles in the energy range  $1 \times 10^{13} \sim 3 \times 10^{15}$  eV and  $3 \times 10^{15} \sim 3 \times 10^{18}$  eV, respectively. Fig. 8 is a contour plot of the number density distribution of re-accelerated CRs ( $E > 3 \times 10^{15}$  eV) (thick lines). In the figure we also plot the distribution of seed particle from SNR (thin lines). We point out that the spatial distributions of seed and re-accelerated CRs in the disk are quite different. In principle, CR distribution can be derived from gamma-ray data.

For instance, Breitschwerdt et al. (2002) used the gradient of gamma-ray emissivity in the disk derived from the EGRET data for the analysis of CR propagation in the Galaxy. If the diffuse gamma-ray data at  $E > 10^{15}$  eV were available, the gradient test would be a nice tool to investigate possible proton sources in this energy range and might lend support to our model.

## 7. Discussions and Final Remarks

We have summarized current understandings about the origin of CRs. It is generally believed that most CRs power can be provided by SNRs. However the CRs with energies  $E > 10^{15}$  eV are quite difficult to achieve in supernovae due to the limited acceleration time and energy content in SN shocks. On the other hand we argue that shocks in the Fermi Bubble produced by stellar capture events can have much longer life time  $> 10^7$  yr and larger energy content  $\sim 3 \times 10^{52}$  erg, which allow them to produce CRs with energies  $E > 10^{15}$  eV. If processes of CR escape from the Galaxy are taken into account, the predicted CR spectrum contributed by the Bubble is  $E^{-\nu}$ , where  $\nu = -\frac{1}{2} + \sqrt{\frac{9}{4} + 10 \frac{(D/3 \times 10^{30} \text{ cm}^2/\text{s})^2}{(u/10^8 \text{ cm/s})^2 (H/10 \text{ kpc})^2}} \sim 3$  for  $10^{15} \text{ eV} < E < 10^{19} \text{ eV}$ . However, it is very difficult to predict the exact value of the spectral index  $\nu$  due to the poorly measured value of diffusion coefficient in the Bubble. So we fit the observed CR spectrum between  $10^{15}$  eV and  $\sim 10^{19}$  eV and find that the diffusion coefficient is about  $3 \times 10^{30} \text{ cm}^2/\text{s}$ . By matching with the observed flux in the knee region we find that the conversion efficiency from shocks in the Bubble to CRs is about 10%, which is quite consistent with numerical simulations. Other input parameters in this model, such as the capture time scale  $\tau_{cap} \sim 3 \times 10^4$  yr, the mean rate of energy release  $\dot{W} \sim 3 \times 10^{40}$  erg/s per capture and the injected wind speed  $u \sim 10^8$  cm/s, have been estimated and used in other observed phenomena in GC (e.g. Cheng et al. 2006, 2007; Dogiel et al. 2009a,b,c, 2011).

We put forth the idea that the Fermi Bubble acts as the re-acceleration site for the CRs produced by SNRs in the Galactic disk. The re-accelerated particles form the part of the observed spectrum that is beyond the “knee” (about  $3 \times 10^{15}$  eV). The part within the “knee” is formed by the CRs produced by the SNRs. We demonstrated this idea by a numerical model. We solve the stationary transport equation in our Galaxy with two Fermi Bubbles (see section 3 for our model of the Bubbles). The re-acceleration process in the Bubble is facilitated by stochastic acceleration. Our model simulated the observed spectrum nicely. Therefore we consider that this model provides a natural explanation about the flux, spectral index and matching at the “knee” of cosmic rays in this energy range.

As described in section 3 there are many many shocks propagating in the Fermi Bubbles. After being re-accelerated inside the Bubbles by the multiple shocks, protons (and nuclei) escape the Bubbles. The life time of proton by pp collision is of the order of  $10^9 \sim 10^{10}$  yr (e.g., Crocker & Aharonian 2011). The diffusion time for protons at these energies to escape the Galaxy is of the order of  $10^7$  yr. Thus after leaving the Bubbles, protons (and nuclei as well) diffuse throughout the whole Galaxy (including the Earth) without any attenuation of energy. Not only protons (and nuclei) can be accelerated by the multiple shocks, but also electrons. Nevertheless, energetic electrons lose energy efficiently. The life time of electrons can be estimated by  $\tau_e = 1/\beta_e E$  (e.g., inverse Compton and synchrotron). Taking  $\beta_e = 3 \times 10^{-25}$  per eV per sec, the life time of electrons of energy  $0.1 \sim 1$  TeV is  $1 \sim 0.1$  Myr. Once they leave the acceleration site (i.e., Fermi Bubbles), they lose most of their energy within a short distance (less than 1 kpc). Hence the electrons are pretty much confined in the Bubbles.

Su et al. (2010) suggested that electron spectrum must be  $E^{-\alpha}$  for  $E < \text{TeV}$  and the spectral index  $\alpha \sim 2.4 - 2.8$ . It is clear that the energy loss processes for protons and electrons are very different, therefore protons and electrons in the Bubble can have different



spectra. In CCDKI model we have assumed that the shocks can produce an injected electron spectrum  $\sim E^{-2}$ , in which the spectrum is modified by processes of energy losses and escape. In our subsequent work we will take into account the stochastic acceleration processes (multiple-shock) to see how the electron spectrum is affected. We will also further analyze the spatial spectral distribution of electrons. Preliminary result can be found in Chernyshov et al. (2011), in which the spatial distribution of gamma ray emission is reproduced nicely by the multi-shock model.

### Acknowledgements

We are very grateful to A.M. Bykov, R.M. Crocker, A.D. Erlykin, Y. Uchiyama and V.N. Zirakashvili for useful discussions, and K.F. Sinkov who performed graphic and numerical illustrations of the Kompaneets' solution presented in section 3. DOC and VAD are partly supported by the NSC-RFBR Joint Research Project RP09N04 and 09-02-92000-HHC-a. KSC is supported by the GRF Grants of the Government of the Hong Kong SAR under HKU 7011/10P. CMK is supported by the Taiwan National Science Council Grants NSC 98-2923-M-008-01-MY3 and NSC 99-2112-M-008-015-MY3. WHI is supported by the Taiwan National Science Council Grant NSC 97-2112-M-008-011-MY3 and Taiwan Ministry of Education under the Aim for Top University Program National Central University.

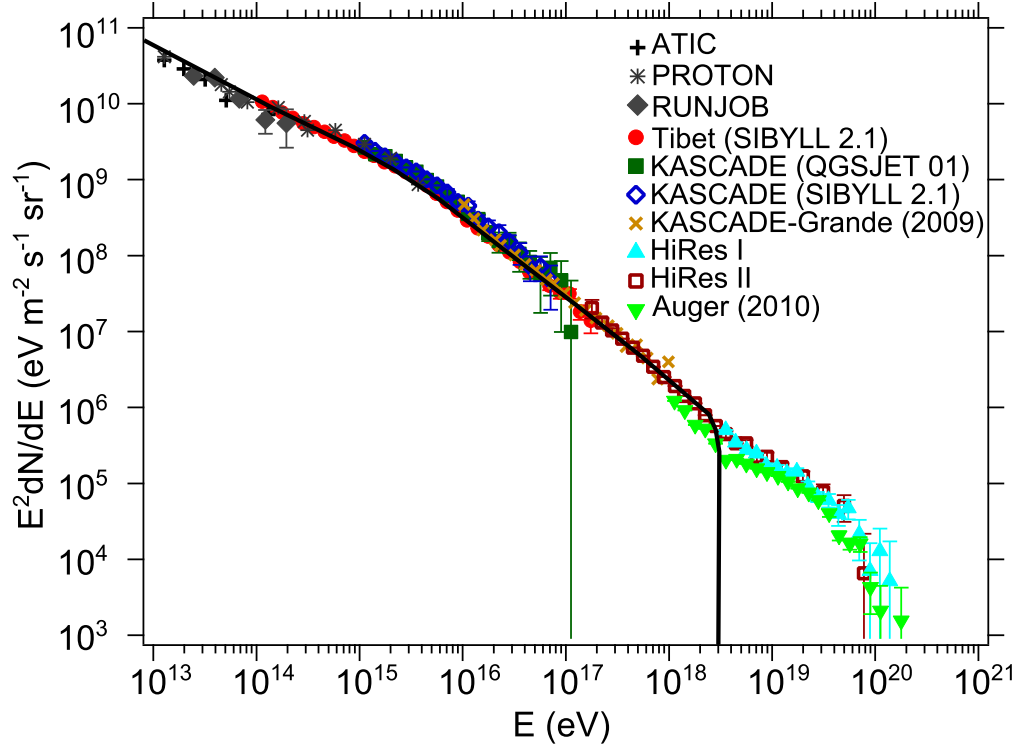


Fig. 5.— CR spectrum at the Earth as a combination of SNR contribution (in the galactic disk) and the stochastic acceleration in the Fermi Bubbles. In addition to data from experiments presented in Fig. 4, we added experiments for lower energies: ATIC (Ahn et al. 2008), Proton (Grigorov et al. 1971) and RUNJOB (Apanasenko et al. 2001). The black solid line is the spectrum from our numerical model. In this model,  $D_B = 2.08 \times 10^{30} \text{ cm}^2/\text{s}$  inside the Bubbles and  $D_G = 6.2 \times 10^{28} (pc/4 \text{ GeV})^{0.6} \text{ cm}^2/\text{s}$  outside,  $\kappa_B H^2/D_B = 1.9$  and the injection spectrum from SNR  $\mu = 4.35$ .

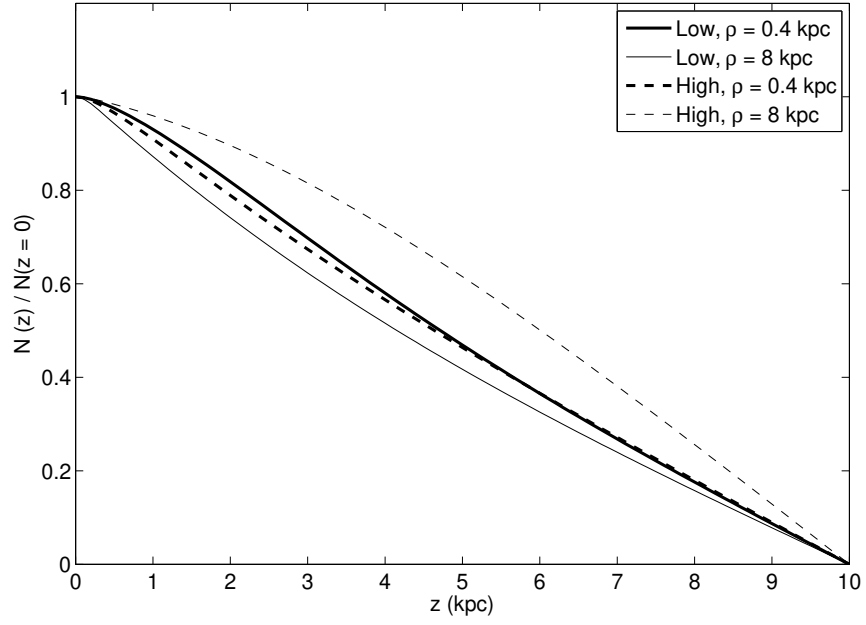


Fig. 6.— The vertical distribution of the number density of CR at two galactocentric radii, 0.4 kpc (thick lines) and 8 kpc (thin lines), in two energy ranges, ‘Low’ for  $1 \times 10^{13} \sim 3 \times 10^{15}$  eV (solid lines) and ‘High’ for  $3 \times 10^{15} \sim 3 \times 10^{18}$  eV (dotted lines).

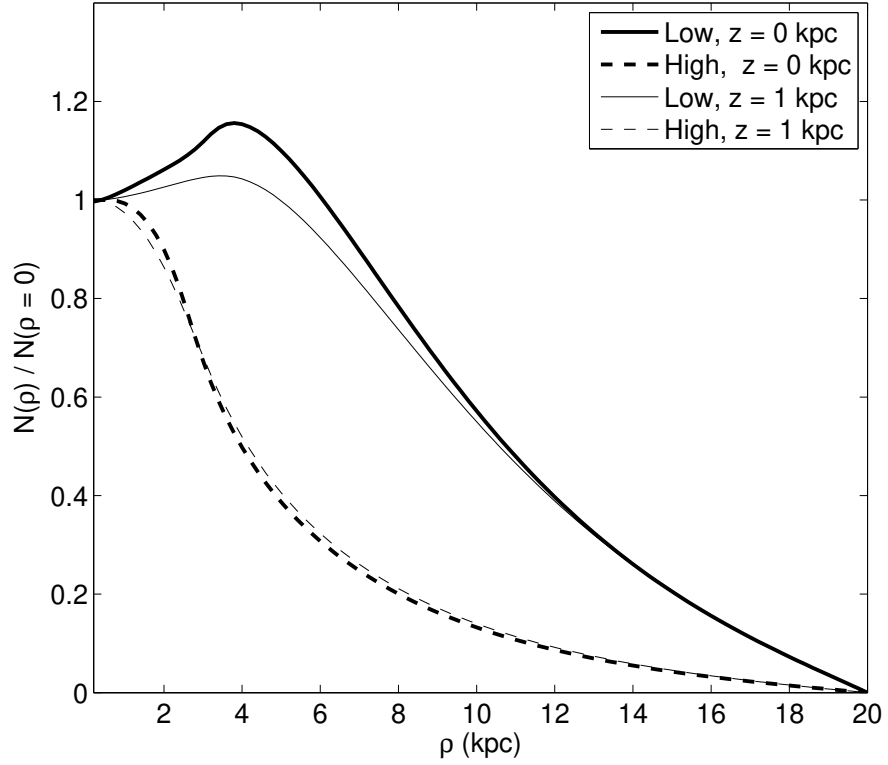


Fig. 7.— The radial distribution of number density of CR at the Galactic plane (thick lines) and 1 kpc above the plane (thin lines), in two energy ranges, ‘Low’ for  $1 \times 10^{13} \sim 3 \times 10^{15}$  eV (solid lines) and ‘High’ for  $3 \times 10^{15} \sim 3 \times 10^{18}$  eV (dotted lines).

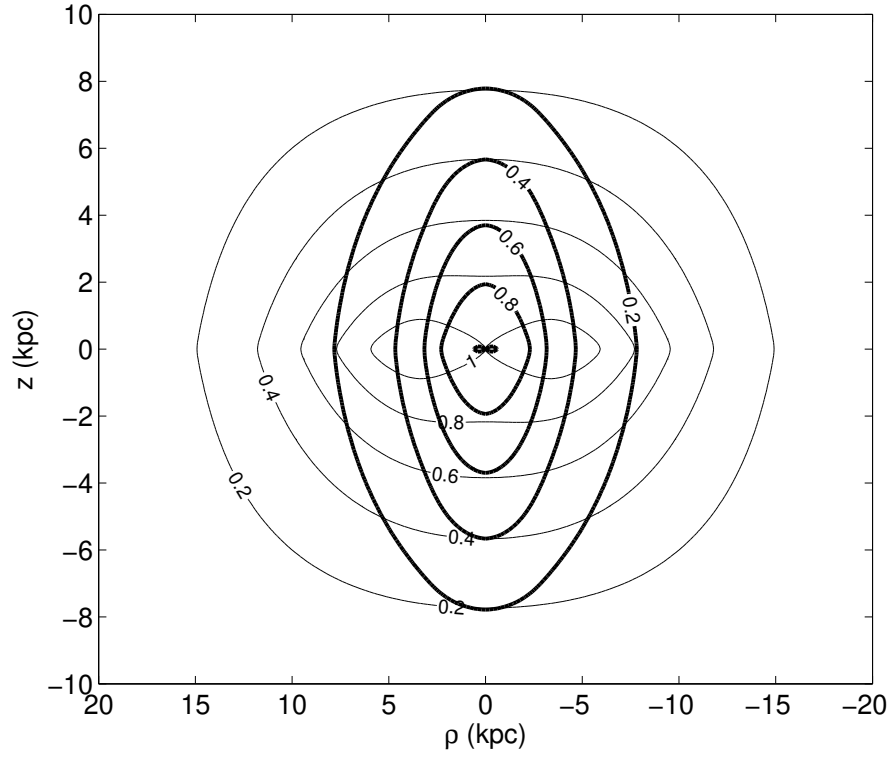


Fig. 8.— The contour of the relative number density distribution of the re-accelerated CRs ( $E > 3 \times 10^{15}$  eV) in the halo (thick lines). The seed for the re-accelerated CRs comes from SNRs in the Galactic plane (thin lines).

## REFERENCES

- Abbasi, R. U. et al. 2008, PRL, 100, 101101
- Abbasi, R. U. et al. 2009, Astroparticle Physics, 32, 53
- Abdo, A. A. et al. 2010, ApJ, 710, L92
- Abraham, J. et al. 2010, Physics Letters B, 685, 239
- Achterberg, A. 1990, A&A, 231, 251
- Aharonian, F., Akhperjanian, A. G., Bazer-Bachi, A. R. et al. 2006, Nature, 439, 695
- Ahn, H. S. et al. 2008, in Int. Cosmic Ray Conf., ed. R. Caballero, J. C. D’Olivo, G. Medina-Tanco, L. Nellen, F. A. Sánchez, J. F. Valdés-Galicia, 2, 79
- Alexander, T. 2005, PhR, 419, 65
- Amenomori, M. et al. 2008, ApJ, 678, 1165
- Apanasenko, A. V. et al. 2001, in Proc. 27th Int. Cosmic Ray Conf., Hamburg, Germany, p. 1622
- Apel, W. D. et al. 2009, in Proc. 31st International Cosmic Ray Conference, Lodz, Poland, arXiv:0906.4007v1 [astro-ph.HE]
- Barthelmy, S. D. et al. 2011, GCN 11824
- Bell, A. R. 1978, MNRAS, 182, 147 and 443
- Bell, A. R. 2004, MNRAS, 353, 550.
- Berezhko, E. G., Yelshin, V. K. & Ksenofontov, L. T. 1994, Astroparticle Physics, 2, 215
- Berezhko, E. G. & Völk, H. J. 2000, A&A, 357, 283

- Berezinskii, V. S., Bulanov, S. V., Dogiel, V. A., Ginzburg, V. L. & Ptuskin, V. S. 1990, *Astrophysics of Cosmic Rays*, ed. V.L.Ginzburg, (Norht-Holland, Amsterdam)
- Biermann, P. L., & Strom, R. G. 1993, A&A, 275, 659
- Bisnovatyi-Kogan, G. S. & Silich, S. A. 1995, RvMP, 67, 661
- Bland-Hawthorn, J. & Cohen, M. 2003, ApJ, 582, 246
- Bloom, J. S. et al. 2011, Science, 333, 203
- Bogdan, A. & Gilfanov, M. 2010, MNRAS, 405, 209
- Breitschwerdt, D., Dogiel, V. A. & Völk, H. J. 2002, A&A, 385, 216
- Bulanov, S. V., Dogel, V. A. & Syrovatskij, S. I. 1972, Cosmic Research, 10, 478
- Bulanov, S. V. & Dogel, V. A. 1974, ApSS, 29, 305
- Burrows, D. N. et al. 2011, Nature, 476, 421
- Butt, Y. 2009, Nature, 460, 701
- Bykov, A. M. & Fleishman, G. D. 1992, MNRAS, 255, 269
- Bykov, A. M. & Toptygin, I. N. 1993, Physics Uspekhi, 36, 1020
- Bykov, A. M. & Toptygin, I. N. 2001, Astronomy Letters, 27, 625
- Bykov, A. M., Osipov, S. M. & Toptygin, I. N. 2009, Astronomy Letters, 35, 555
- Cannizzo, J. K., Lee, H. M. & Goodman, J. 1990, ApJ, 351, 38
- Cappelluti, N. et al. 2009, A&A, 495, 9
- Caprioli, D. 2011, J. Cosmology and Astroparticle Phys., 5, 26

- Castro, D. & Slane, P. 2010, *ApJ*, 717, 372
- Cenko, S. B. et al., 2011, GCN 11827
- Cheng, K.-S., Chernyshov, D. O. & Dogiel, V. A. 2006, *ApJ*, 645, 1138.
- Cheng, K.-S., Chernyshov, D. O. & Dogiel, V. A. 2007, *A&A*, 473, 351.
- Cheng, K.-S., Chernyshov, D. O., Dogiel, V. A., Ko, C.-M. & Ip, W.-H. 2011, *ApJ*, 731, L17 (CCDKI)
- Chernyshov, D. O., Cheng, K.-S., Dogiel, V. A., Ko, C.-M., Ip, W.-H. & Wang, Y. 2011, arXiv:1109.2619v1 [astro-ph.GA]
- Cordes, J. M., Weisberg, J. M., Frail, D. A. et al. 1991, *Nature*, 354, 121
- Crocker, R. M. & Aharonian, F. 2011, *PRL*, 106, 101102
- Crocker, R. M., Jones, D. I., Aharonian, F. et al. 2010, *MNRAS*, 411, L11
- Cummings, J. R. et al., 2011, GCN 11823
- de Almeida, U. B. & De Angelis, A. 2011, arXiv:1104.2528v2 [astro-ph.HE]
- Dogiel, V. A., Cheng, K.-S., Chernyshov D. et al. 2009a, *PASJ*, 61, 901
- Dogiel, V. A., Chernyshov D., Yuasa, T. et al. 2009b, *PASJ*, 61, 1099
- Dogiel, V. A., Tatischeff, V., Cheng, K.-S. et al. 2009c, *A&A*, 508, 1
- Dogiel V. A., Chernyshov, D., Koyama, K., Nobukawa, M. & Cheng, K.-S. 2011, *PASJ*, 63, 535
- Erlykin, A. D. & Wolfendale, A. W. 2006, *JPhG*, 32, 1



- Erlykin, A., Wibig, T., & Wolfendale, A. W. 2011, *Astrophysics and Space Sciences Transactions*, 7, 179
- Esquej, P. et al. 2008, *A&A*, 489, 543
- Finkbeiner, D. P. 2004, *ApJ*, 614, 186
- Gezari, S. et al. 2008, *ApJ*, 676, 944
- Gezari, S. et al. 2009, *ApJ*, 698, 1367
- Greene, J. E. & Ho, L. C. 2007, *ApJ*, 667, 131
- Grigorov, N. L. et al. 1971, in *Proc. 12th Int. Cosmic Ray Conf.*, Hobart, Australia, 5, 1746
- Guo, F. & Mathews, W. G. 2011, arXiv:1103.0055v1 [astro-ph.HE]
- Guo, F., Mathews, W. G., Dobler, G. & Oh, S. P. 2011, arXiv:1110.0834v1 [astro-ph.HE]
- Halpern, J. P., Gezari, S. & Komossa, S. 2004, *ApJ*, 604, 572
- Inui, T., Koyama, K., Matsumoto, H. & Tsuru, T.G. 2009, *PASJ*, 61, S241
- Ip, W.-H. & Axford, W. I. 1992, *AIP Conference Proceedings* 264 (Eds. G. P. Zank and T. K. Gaisser), 264, 400
- Jokipii, J. R. & Morfill, G. 1987, *ApJ*, 312, 170
- Jones, F. C., Lukasiak, A., Ptuskin, V. & Webber, W. 2001, *ApJ*, 547, 264
- Kampert, K.-H. et al. 2004, *Nuclear Physics B Proceedings Supplements*, 136, 273
- Knoedlseder, J., Jean, P., Lonjou, V. et al. 2005, *A&A*, 441, 513
- Komossa, S. & Bade, N. 1999, *A&A*, 343, 775

- Kompaneets A. S. 1960, Akademiia Nauk SSSR, Doklady (DoSSR, in Russian), 130, 5
- Kotera, K. & Olinto, A. V. 2011, arXiv:1101.4256v1 [astro-ph.HE], doi:10.1146/annurev-astro-081710-102620
- Koyama, K., Hyodo, Y., Inui, T. et al. 2007, PASJ, 59, 245
- Krymskii, G. F. 1977, Akademiia Nauk SSSR, Doklady (DoSSR, in Russian), 234, 1306
- Lagage P. O. & Cesarsky, C. J. 1983, A&A, 125, 249.
- Lagutin, A. A., Tyumentsev, A. G. & Yushkov, A. V. 2008, NuPhS, 175, 555
- Landau, L. D. & Lifshitz, L.M. 1991, Quantum mechanics non-relativistic theory, 3rd ed., Pergamon
- Leloudas et al., 2011, GCN 11830
- Levan, A. J. et al. 2011a, GCN 11833
- Levan, A. J. et al. 2011b, Science, 333, 199
- Magorrian, J. et al. 1998, AJ, 115, 2285
- Melrose, D. B. & Pope, M. H. 1993, PASAu, 10, 222
- Ponti, G., Terrier, R., Goldwurm, A. et al. 2010, ApJ, 714, 732
- Ptuskin, V. S., Rogovaya, S. I., Zirakashvili, V. N. et al. 1993, A&A, 268, 726
- Ptuskin V., Zirakashvili, V. & Seo, E.-S. 2010, ApJ, 718, 31
- Rees, M. J. 1988, Nature, 333, 523
- Reynolds, S. P. 2008, ARAA, 46, 89

- Schneider, P. 1993, *A&A*, 278, 315
- Spruit, H. 1988, *A&A*, 194, 319
- Stecker F. W., & Jones, F. C. 1977, *ApJ*, 217, 843
- Strong, A. W. & Moskalenko, I. V. 1998, *ApJ*, 509, 212
- Su, M., Slatyer, T. R., & Finkbeiner, D. P. 2010, *ApJ*, 724, 1044
- Syer, D. & Ulmer, A. 1999, *MNRAS*, 306, 35
- Syrovatskii S. I. 1971, *Comm. Ap. Sp. Phys.*, 3, 155
- Terrier, R., Ponti, G., Belanger, G. et al. 2010, *ApJ*, 719, 143
- Tremaine, S. et al. 2002, *ApJ*, 574, 740
- Uchiyama, Y. 2011, arXiv:1104.1197v1 [astro-ph.HE]
- Weaver, R., McCray, R., Castor, J., Shapiro, P. & Moore, R. 1977, *ApJ*, 218, 377
- Webb, G. M., Ko, C. M., Zank, G. P. & Jokipii, J. R. 2003, *ApJ*, 595, 195
- Zauderer, B. A. et al. 2011, *Nature*, 476, 425